MET'2015 Croatia
Trogir, October 4 - 7, 2015
12th International Conference
Modern Electrified Transport

ANALYSIS OF MEASUREMENT AND SIMULATION RESULTS OF FREIGHT TRAIN POWER SUPPLY

Milivoj Mandić [1], Viktor Milardić[2], Ivo Uglešić [2], Božidar Filipović-Grčić [2]
[1]Croatian Railways Infrastructure[2], Faculty of Electrical Engineering and Computing, University of Zagreb, Croatia

Abstract
After modifying the power supply system on the railway section it was put into test operation. One freight train was driven along section and current and voltages measurements were conducted in each electric traction substation.
The obtained measurement results were analysed and compared with the simulation results of the developed software for train movement simulation. Maximum simulated results deviate from the maximum measurement results in the range of 3.2% in the worst case scenario. Maximum observed deviations between simulation and measurement results do not exceed 17.8%.

1. Introduction

In the planning/design of new railway lines, electrification or modification of power supply of the existing railway lines [1], the planned increase in transportation (increase the flow of railway lines, increasing the weight of the trains, the introduction of new locomotives with greater tensile power), the question is the appropriate infrastructure for power supply. The infrastructure for power supply of the 50 Hz AC railway system consists of electric traction substations (ETS), contact network (CN) and sectioning facilities, [2]. To determine the optimum position and installed power of the ETS it is necessary to:

1. Simulate the movement of trains, at any time, based on a planned timetable, to determine the position of trains and the active and the reactive power taking from the CN;
2. Calculate the present value of current and voltage in the contact network, apparent power load of ETS, apparent mean 15 minutes power, active power, reactive power, power factor l, heating (over temperature) of the contact wire etc. [2].

Estimation of energy consumption for electric trains is widely applied to the planning/design of power supply systems and the study of optimal driving strategies. Research on optimal driving strategies requires higher precision than power system planning/design since the latter usually takes the worst case scenario to consider safe margins.

Train movement simulation and the calculation of electric situation in the traction power supply system are the problems which are practiced by many authors, [3], [4],. In [5] Majumdar proposed four main stages of train movement including (1) acceleration, (2) balancing, (3) coasting and (4) deceleration. He showed that the total energy consumed in train operations is the product of force and displacement. He used coefficients for converting the work done in ton-km into electric power units. Majumdar also proposed a statistical method for estimating energy. In [6] Goodman developed single train and multi train simulation programs.

The voltage received by a train will vary with position and the simultaneous action of other trains in multi train model, while it remains a constant in a single train model. This is the main difference between two models in estimating energy consumption. Goodman considered detailed factors in his model, including substation, feeder cable and volt-drop, etc. In [7] the design of an electric train network simulator is described. The proposed software aims to help designing electric train power supply networks. It consists of two combined simulators namely a run time simulator and a network simulator. There are also commercial software for train movement simulation and the calculation of electric situation in the traction power supply system, [8], [9]. Many authors have studied the problem of energy consumption for electric traction. In [10] Martin discussed simulation in general. He showed 5% extension on run time can produce energy savings up to 20% on a suburban system, similar as in [11]. In [12] author developed a model which estimates power consumption at high precision with 2% deviation from a real situation. It is found that reducing maximum speed and tactfully performing coasting can reduce energy consumption about 7% ~ 20%. In [13] two models for estimating energy consumption of single train operation are presented. Paper [14] describes the work of simulating and analysing dynamic traction power supply system. It is based on dependent train movement in conjunction with traction power supply system simulation to establish a panorama view of the features.

This paper describes new software developed for train movement simulation and a comparison of simulation results with measurements.

1.1. The section where the measurements were conduced

On the observed section, modernization of the railway system has been recently implemented, the transition from the outdated 3 kV DC system on single-phase AC 25 kV 50 Hz. This railway line connects the port city with major transport junction and its main function is cargo transport. By modifying the railway traction system its carrying capacity is increased from 6 to 10 million net tons per year. Figure 1 shows conditions of the observed section, at the time of measurement, the number and position of ETS and sectioning facilities as well as the terrain configuration.

The observed railway section was put into test operation and current and voltage measurements in each ETS were performed. The results of measurements, carried out in all three ETS, have been compared with simulation results of the developed software.

Commissioning of the modernized railway section created a unique opportunity to obtain the most accurate measurement results. The reason for this is reduction of the impact of other trains that normally travel on the observed section, [15]. This was achieved by travelling of one test freight train along the whole supply area of each ETS.

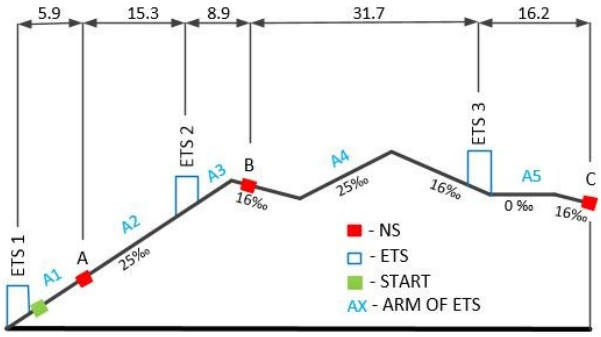

Fig. 1. Terrain configuration of the observed section

2. Train movement simulator

Train movement simulator for electrified railways was developed in Microsoft Visual Studio programming language C#. The purpose of this simulator is to calculate the position of the train, amount of active (P) and reactive (Q) power taken by locomotive from CN at a particular time interval. The input data necessary for such calculation are profile of railway lines, the planned speed on each section and the characteristics of the locomotive and train.

2.1. Physical representation of train movement

Different driving resistance appear during the train movement. For train movement, the pulling force on the perimeter of the drive wheels must be equal to the sum of all resistances. Calculation of individual resistance components is very complex and empirical expressions are usually used, which are commonly polynomials of speed in form:

$$F_p = A \cdot v^2 + B \cdot v + C \tag{1}$$

The coefficients A, B and C depend on the type and composition of the train, and can take different in different countries. We are using Strahl formulas, in which specific resistance are calculated values separately for locomotive and for train. Expressions are given below, f_{vv} for locomotive and f_{vi} for train.

$$f_{vv} = \left(20 + \frac{v^2}{240}\right) \cdot 10^{-3} \left[\frac{N}{kg}\right] \tag{2}$$

$$f_{vi} = \left(20 + k \cdot \frac{v^2}{10}\right) \cdot 10^{-3} \left[\frac{N}{kg}\right] \tag{3}$$

In previous expressions (2 and 3) speed is expressed in km/h, and value of the coefficient k in (3) depends on the type of train. Dependence is shown in Table 1.

Table 1. Dependence of coefficient k on train type

Train type	k
Fast passenger train	0.032
Passenger train	0.04
Fast freight train	0.047
Medium weighted freight train	0.057
Empty freight train	0.108

2.2. Calculation of active and reactive power

Knowing the necessary traction force to achieve the movement, it is possible to calculate the mechanical force on the perimeter of the wheel through the following expressions:

$$P_m = F_t \cdot v \tag{4}$$

To calculate active power, which locomotive takes from CN it is necessary to know the efficiency of the locomotive (h) that depends on the speed and supply voltage of the CN. Active power that locomotive takes from CN (P_{el}) is calculated using the expression:

$$P_{el} = \frac{P_m}{\eta} + P_{pom} \tag{5}$$

Where P_{pom} is auxiliary power (wagon heating, engine cooling, etc.). In the case of AC power supply, locomotive takes the active and reactive power from CN. The reactive power is calculated according to the formula:

$$Q_{el} = P_{el} \cdot \tan(\arccos(\cos \varphi)) \tag{6}$$

Displacement factor ($\cos \varphi$ is dependent on the speed of the train. Some locomotive generate higher harmonics, which, along with reactive power of the operating frequency, contribute to an increase in total required reactive power. Therefore in the calculation, instead of the displace-

ment factor power factor λ is used, which takes into account the occurrence of reactive power due to the higher harmonics. Factor λ is dependent on the vehicle speed and the λ -curve for locomotives of series 141 and 142 are shown in Figure 2. Factor λ is particularly important when calculating traffic with frequent starting and stopping, because at lower speed, factor λ is also lower and the engaged reactive power is greater.

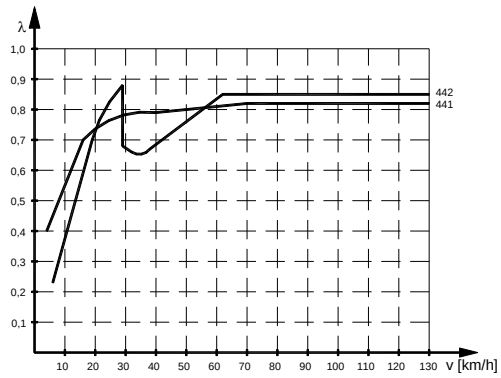

Fig. 2. λ factor depending on the speed of the locomotive 141 and 142

2.3. Calculation of active and reactive power

If at time *t*, the train speed and its position on the railway lines is known, the driving resistance and adhesion force can be calculated and possible traction force of locomotive determined, which depends on the regime of the train movement. Based on the known traction force and speed at time *t*, mechanical power can be calculated followed by calculation of active and reactive electric power. If the train accelerates, the acceleration is being calculated, and then increase of speed and time. The procedure is repeated for the next time interval D*t*- calculation step l.

3. Results of measurement

Measurement of electric conditions was carried out in three ETS.

Example 1. ETS1

In all ETSs two transformers of a rated power of 10 MVA or 7.5 MVA and with a transmission ratio of 110/27.5±10x1.5% were installed, as well as a capacitor bank that has a possibility of reactive power regulation in six degrees in the no-load condition.

The test freight train of total mass of 800 t was travelling along the observed section of railway track, which is shown in Table 2. The train departed from the station ST-3 at 10:08 AM and was travelling in the area supplied by ETS1 till 11:39 AM. The measuring results recorded in that period are shown next.

Table 2. Overview of test freight train movement in the area supplied by ETS1

TRAIN STATION	ARRIVAL (HH:MM)	DEPARTURE	DELAY (MM:S)
ST-3	-	10:08	08:00
ST-2	10:26	10:55	09:00
ST-1	11:39	-	39:20

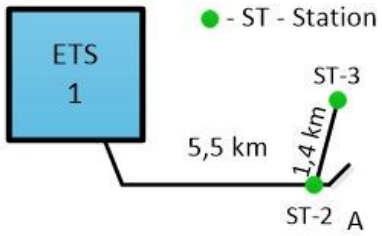

Fig. 3 . Power supply scheme of ETS1

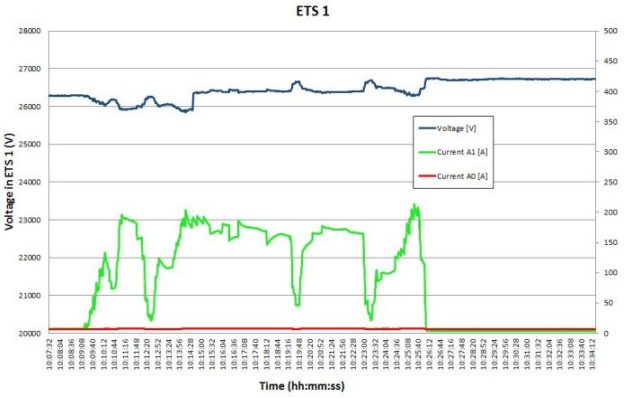

Fig. 4. Voltage and current in ETS1 during the movement of test freight train (800 t)

From Fig. 4. it is evident that current does not exceed the value of 220 A at maximum load. Voltage oscillations range in values of 25.9 kV to 27.5 kV given that the mentioned values are in permanently permissible limits, according to EN50163 (Table 3.). It can be concluded that during the entire period of investigation stable voltage conditions were present.

Example 2. ETS3

The test freight train of total mass of 788 t was travelling along the observed railway track section, which is shown in Table 3. The train was travelling in the area supplied from ETS3 from 11:45 AM till 12:52 PM. The measuring results recorded in that period are shown next.

Table 3. Overview of test freight train movement in the area supplied by ETS1

TRAIN STATION	ARRIVAL (HH:MM)	DEPARTURE (HH:MM)	DELAY (MM:S)
ST-5	11:45	11:45	-
ST-6	11:55	12:11	00:20
ST-7	12:23	12:23	-
ST-8	12:31	12:31	
ST-9	12:39	12:39	-
ST-10	12:47	12:52	00:07

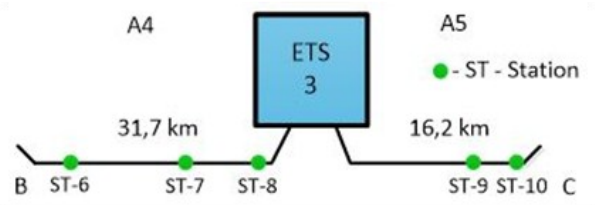

Fig. 5. Power supply scheme of ETS3

During the train ride, along the entire supply area of ETS3, voltage oscillations range in values of 25.96 kV to 27.16 kV (Fig. 16). According to the norm EN50163, it can be concluded that during the entire period of investigation stable voltage conditions were present.

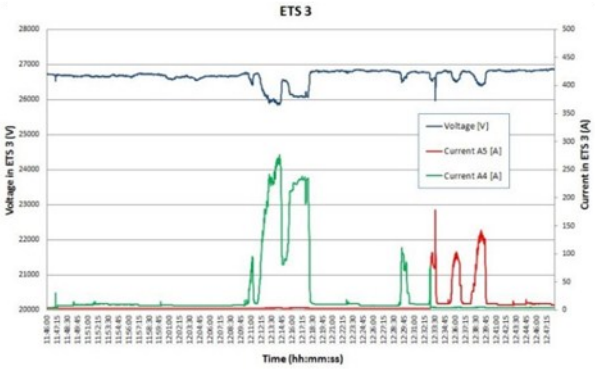

Fig. 6. ETS3 – measurement results of voltage and current

From Fig. 6 it is evident that current does not exceed the value of 275 A at maximum load.

4. Comparison of simulation and measurement

The train movement simulator was used in order to calculate the electrical conditions during the movement of the test freight train.

Example 1. ETS1

Results of measuring current, active and reactive power together with simulation results as a function of time for movement test freight train in the supply area of ETS1 are shown in Figure 7.

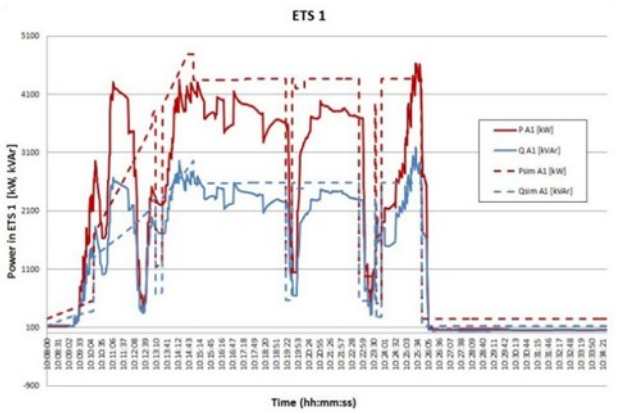

Fig. 7. Comparison of measurement and simulation results of the freight train moving along the supply branch A1

The test freight train which was pulled by two locomotives consumed the maximum active power in the amount of 4.6 MW and the maximum reactive power of 3.2 MVAr from the CN while accelerating up to the prescribed limit. (Fig. 13.)

Deviation of simulation results and actually measured maximum values of active power are 3.2% and 8.84% for reactive power.

Example 2. ETS3

a) The movement of train along the branch A4

The test freight train, total mass of 788 t, was moving constantly downhill along the branch A4. During that period it was taking energy from the CN which is equivalent to energy of auxiliary drives and energy required for breaking. Measurement results have shown that the real values were close to the assumed values in a simulator. (Fig. 8.) Values of active power are in range 50 to 75 kW and values of reactive power are in range 40 to 65 kVAr.

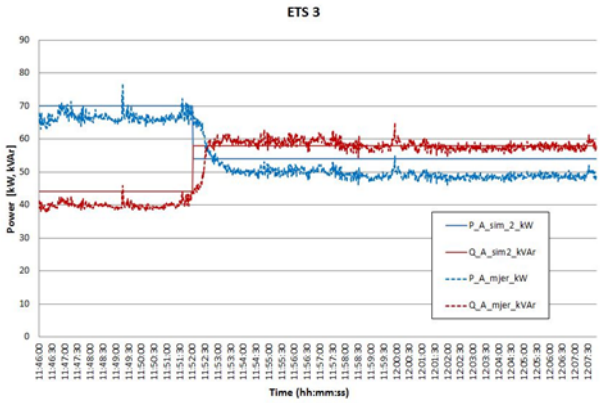

Fig. 8. Comparison of measurement and simulation results of the freight train moving along the supply branch A4

b) The movement of train along the branch A5

Along the branch A5 the train was also constantly moving downhill, during that period of time it was taking energy

from the CN which is equivalent to the energy of auxiliary drives and energy required for breaking. Measurement results are shown in Fig. 17.

In Fig. 9. we can see a peak when train takes from CN active power in amount of 420 kW and reactive power in amount of 320 kVAr. This is the moment when the train departs from station, releases the brakes and starts to accelerate downhill.

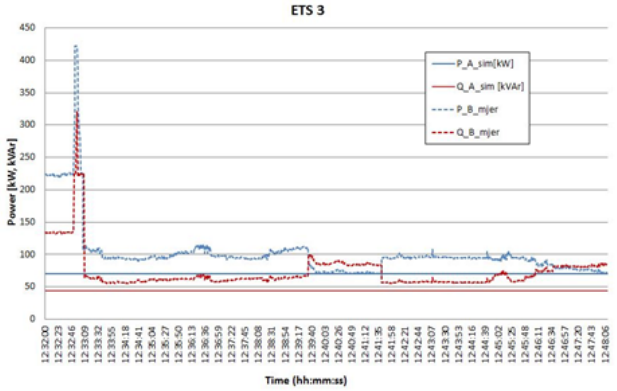

Fig. 9. Comparison of measurement and simulation results of the freight train moving along the supply branch A5

5. Electric locomotives with diode rectifiers – influence on power quality in transmission network

Majority of electric locomotives in Croatian electric railway system 25 kV, 50 Hz are equipped with DC motors and diode rectifiers. Diode rectifier bridge causes current waveform distortion and as a consequence voltage distortion in transmission power system.

Diode locomotive consists of an autotransformer, diode rectifiers and four DC motors. The autotransformer 25/1.06 kV connects contact wire with diode rectifiers and DC motors. Figure 10 shows the electrical scheme of diode locomotive.

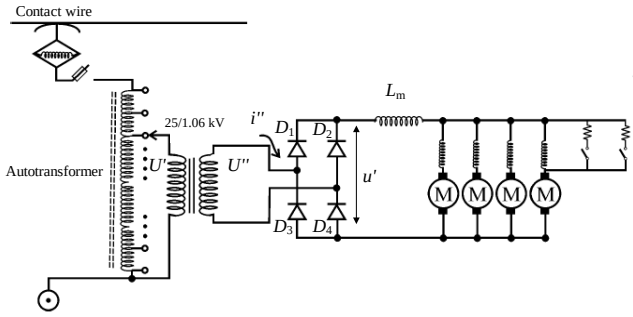

Fig.10. Electrical scheme of the diode locomotive

Figure 11 shows voltage *U*'' and current *i*'' waveforms entering the diode rectifier. Diode rectifier has one commutation over one semi-period of voltage. The Figure 11 also shows conducting sequence of individual diodes in the rectifier bridge as well as commutation when all diodes simultaneously conduct in a short time period (in Fig. 11 this time period is enlarged). Odd current harmonics (3rd, 5th, 7th, 9th,…) are characteristic for diode bridge rectifiers.

5.1. Modeling of electric railway system

A model of electric railway system connected to 110 kV network was developed in order to determine power quality parameters of voltage and current. A model consists of electric railway substation and contact line feeding electric locomotives equipped with diode rectifiers. Figure 12 shows the model in EMTP-RV software which is used for analysis of electromagnetic transients.

An electric railway substation consists of one 110/25 kV transformer with rated power 7.5 MVA which is connected to the transmission grid. The transformer impedance was calculated from the manufacturer data.

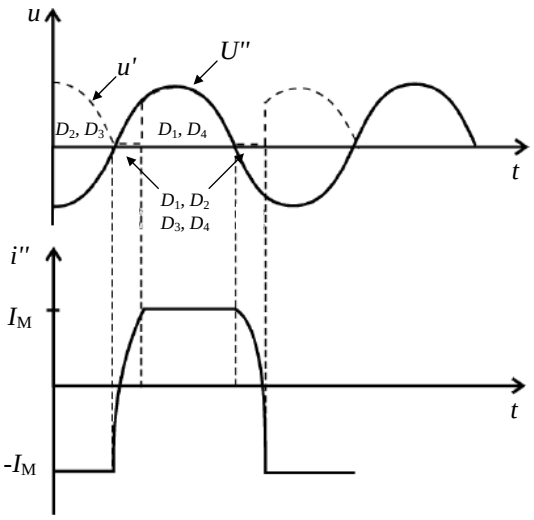

Fig. 11. Diode rectifier voltage and current waveforms

110 kV transmission network is represented by Thevenin equivalent (impedance in series with voltage source). The positive and zero sequence impedance was calculated from single-phase and three-phase short-circuit currents.

The catenary system was modeled using a frequency-dependent J. Marti model which is based on the approximation of the line characteristic impedance $Z(\omega)$ and propagation function $A(\omega)$ by rational functions of the higher order. Ground resistivity was assumed 100 Ωm. Figure 13 shows a 25 kV catenary system which consists of a messenger wire and contact wire. The parameters of the catenary system are shown in Table 4.

DC motor model consists of main field inductance, armature and commutating pole resistance and back electromotive force.

Regarding the rectifier bridge it is represented with the series resistance of the diodes and the parallel RC elements. To smooth the direct current a series reactor is connected between the rectifier bridge and the motor. This reactor together with its resistance was also taken into account in calculations.

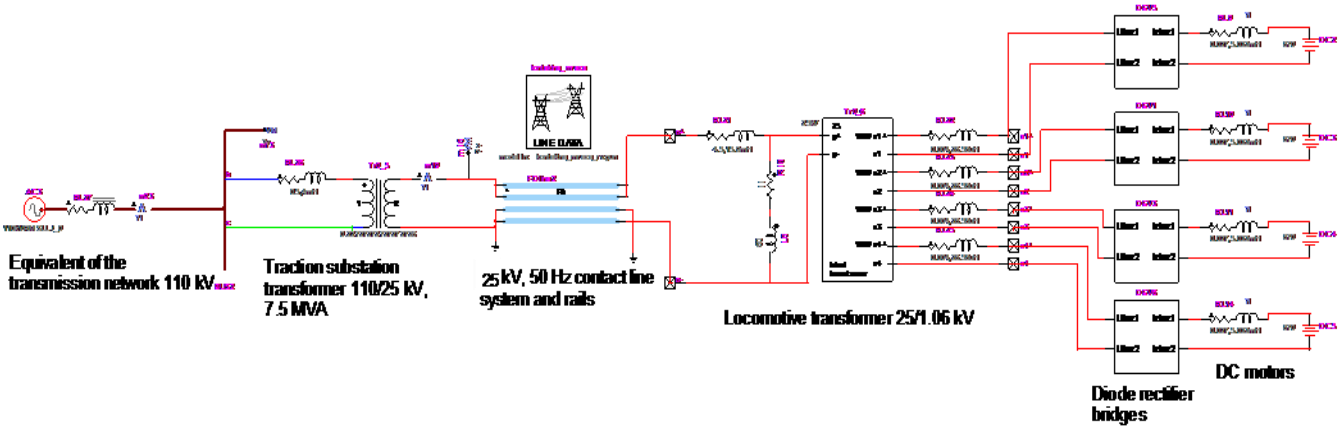

Fig. 12. EMTP-RV model of an electric railway system

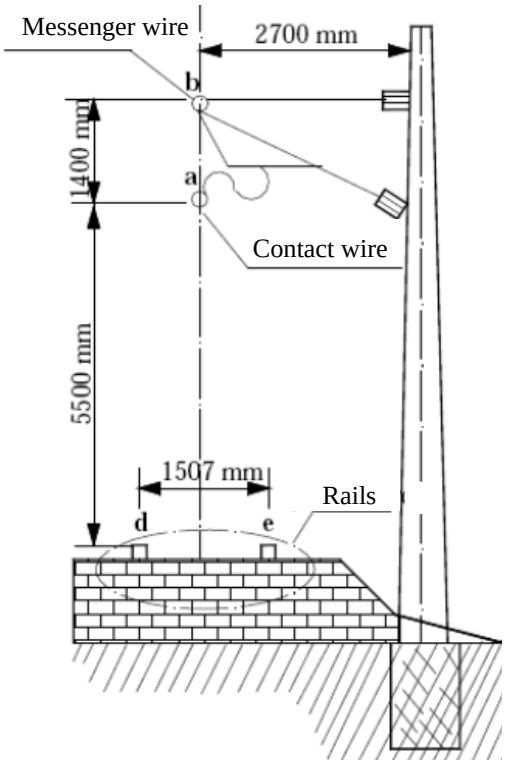

Fig. 13. Configuration of the 25 kV, 50 Hz catenary system

Table 4. Parameters of the catenary system

	Contact wire	Messenger wire
DC resistance (Ω/km)	0.1759	0.153
Radius (mm)	6	6.18
Cross section (mm^2)	100	120

Diode rectifier bridge is shown in Figure 14

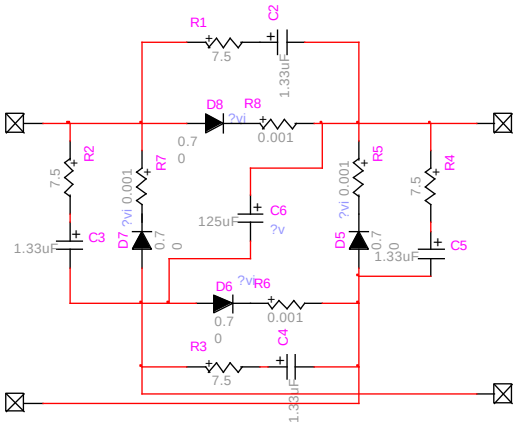

Fig. 14. Diode rectifier bridge

5.2. Analysis of the simulation results

Constant speed of the diode locomotive was analysed. Electric railway system is connected between phase L2 and L3 of the 110 kV network. All calculated values relate to the single diode locomotive 1 km away from the electric railway substation. Voltage and current waveforms were calculated on 25 kV and 110 kV level at the railway substation.

The diode electric locomotive causes voltage distortion in the 25 kV catenary system. Figure 15 shows voltage waveform and Figure 16 current waveform on 25 kV side of railway substation transformer.

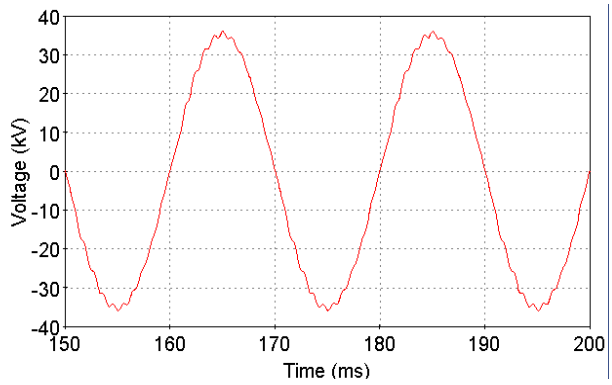

Fig. 15. Voltage waveform on 25 kV side of railway substation transformer

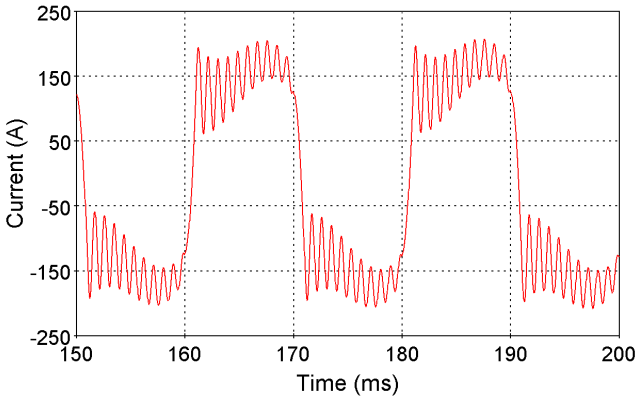

Fig. 16. Current waveform on 25 kV side of railway substation transformer

Figure 17 shows voltage waveform and Figure 18 voltage harmonic spectrum at 110 kV side of railway substation transformer.

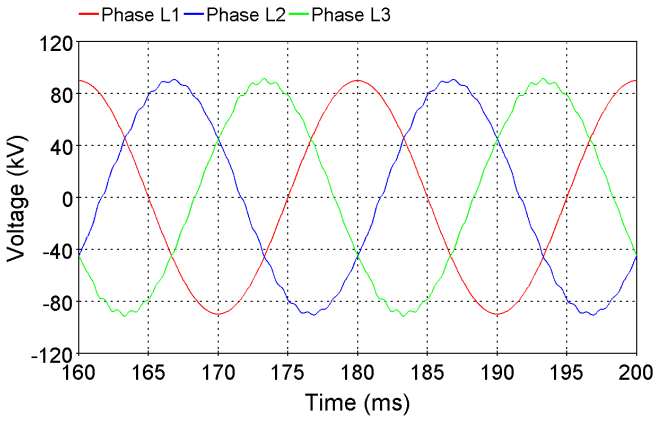

Fig. 17. Voltage waveform at 110 kV side of railway substation transformer

The voltage and current harmonics in 25 kV catenary system is shifted through 110/25 kV transformer in electric traction substation to the 110 kV voltage level.

There is a significant part of higher odd harmonics (23rd and 21st harmonic are the highest). Figure 19 shows current waveform and Figure 20 current harmonic spectrum at 110 kV side of railway substation transformer. The harmonic distortion of 110 kV voltage is significant only in L2 and L3 phases to which the electric railway system is connected.

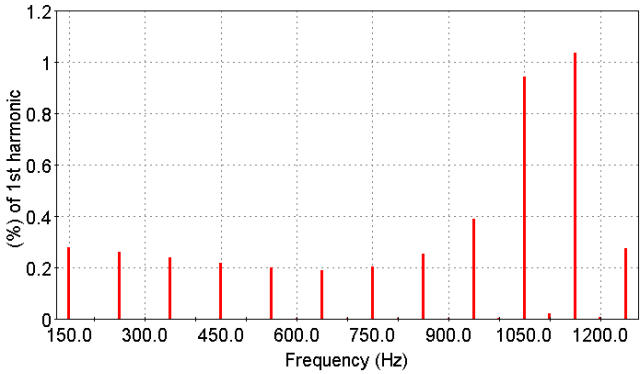

Fig. 18. Voltage harmonics at 110 kV side of railway substation transformer

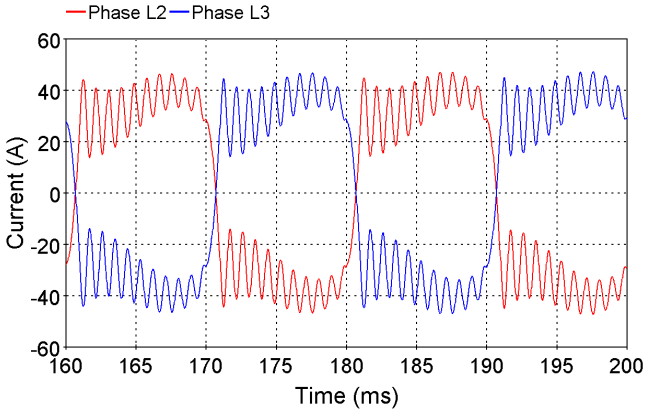

Fig. 19. Current waveforms on 110 kV side of railway substation transformer

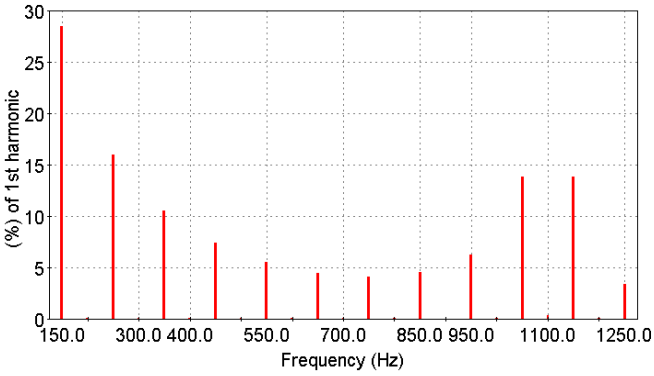

Fig. 20. Current harmonics on 110 kV side of railway substation transformer

The 3rd, 5th, 21st and 23rd harmonic contribute the most to the total current distortion.

Simulations showed that total harmonic distortion (THD) of voltage and current is the highest at the point of connection of the locomotive to contact line. Calculated current and voltage THD at 110 kV and 25 kV level is shown in Table 5.

Table 5. Current and voltage THD at 110 kV and 25 kV level

Voltage	THD *U*	THD *I*
110 kV	1.63 %	41.83 %
25 kV	2.06 %	

6. Conclusions

Software, partly shown in this paper is primarily intended for designing electric traction infrastructure. Maximum simulated results deviate from the maximum measurement results of all 3.2% in the worst case scenario. Maximum observed deviations between simulation and measurement results do not exceed 17.8%. By comparing the simulation and measurement, the results show how developed software works quite well for the intended purpose.

Electric traction, besides representing unbalanced load (compound in two phases of 110 kV network) also affects on the voltage quality in the 110 kV network due to non-sinusoidal currents which diode locomotives take from the network.

7. Future work

Further development of the present software goes in the direction of the simultaneous simulation of the train movement and the traction load flow calculation.

This will take into account the value of the voltage centenary in each train and the influence of the voltage to the speed-traction effort curve.

Acknowledgement

This work has been supported in part by the Croatian Science Foundation under the project "Development of advanced high voltage systems by application of new information and communication technologies" (DAHVAT).

References

1. Jonaitis J. Determination of extreme train running parameters along a railway line segment. *TRANSPORT-2006, vol*. XXI, No. 2, 123-130.
2. Uglešić, I; Mandić, M.; Milardić, V. Design and testing of 25 kV 50 Hz traction power system, Modern electric traction: power supply. Gdansk University of Technology, 2009. pp. 3-13.
3. KePing Li, ZiYou Gao. An improved car-following model for railway traffic. Journal of Advanced Transportation, Volume 47, Issue 4, June 2013, Pages: 475–482.
4. Shinya Kikuchi. A simulation model of train travel on a rail transit line. Journal of Advanced Transportation, Volume 25, Issue 2, Summer 1991, pages 211–224.
5. Majumdar J. The Economics of Railway Traction, Gower, 1985.
6. C. J. Goodman, B. Mellitt, N. B. Rambukwella. CAE for the electrical design of urban rail transit systems, Published in book: Computers in railway operations, pp 173-193, Springler-Verlag New York, 1987.
7. Ruelland F. Electrical Train Network Simulation with a Voltage Booster, 25th IEEE Canadian Conference on Electrical & Computer Engineering (CCECE) April 29 – May 2, 2012, Montreal, Quebec.
8. A. Nash, D. Huerlimann, Railroad Simulation Using OpenTrack, www.opentrack.ch
9. Train, Rail system traction power and performance simulator, www.mottmac.com
10. P. Martin, Train Performance and Simulation, Proceedings of the 1999 Winter Simulation Conference, Vol. 2, pp. 1287-1294. 5-8. December 1999, Squaw Peak, Phoenix, AZ.
11. M. Mandić, I. Uglešić, V. Milardić. Method for Optimization of Energy Consumption of Electrical Trains. I.R.E.E. Vol. 6, N. 1. Jan-Feb 2011; pp. 292-299.
12. T. Norio. Development of Algorithm to Calculate Energy Saving Train Performance Curve, Railway Technology Avalanche, No. 3. August 1, 2003.
13. J-Ch. Jong, E-F Chang. Models for Estimating Energy Consumption of Electric Trains, Journal of the Eastern Asia Society for Transportation Studies, Vol. 6, pp. 278 -291, 2005.
14. D. Yu, K. L. Lo, X. D. Wang, C. G. Yin, D. L. Huang, Analysis of Dynamic MRTS Traction Power Supply Based on Dependent Train Movement Simulation. In: Proceedings of the 2004 ASME/IEEE Joint Rail Conference, April 6-8, 2004, Baltimore, Maryland, USA, pp. 153-161.
15. Bwo-Ren Ke, Chun-Liang Lin, Hsein-Hung Chien, Improvement of Freight Train Timetable for Single-Track Railway System, Consumer and Control, International Conference, 4. – 6. June 2012.